Science Translational Medicine
AAAS

stm.sciencemag.org/cgi/content/full/11/511/eaaw3781/DC1

# Supplementary Materials for

## Muscarinic acetylcholine receptor regulates self-renewal of early erythroid progenitors

Gaurang Trivedi, Daichi Inoue, Cynthia Chen, Lillian Bitner, Young Rock Chung, Justin Taylor, Mithat Gönen, Jürgen Wess, Omar Abdel-Wahab*, Lingbo Zhang*

*Corresponding author. Email: lbzhang@cshl.edu (L.Z.); abdelwao@mskcc.org (O.A.-W.)

Published 25 September 2019, *Sci. Transl. Med.* **11**, eaaw3781 (2019)
DOI: 10.1126/scitranslmed.aaw3781

**The PDF file includes:**

**Other Supplementary Material for this manuscript includes the following:**

(available at stm.sciencemag.org/cgi/content/full/11/511/eaaw3781/DC1)

**Supplementary Materials:**

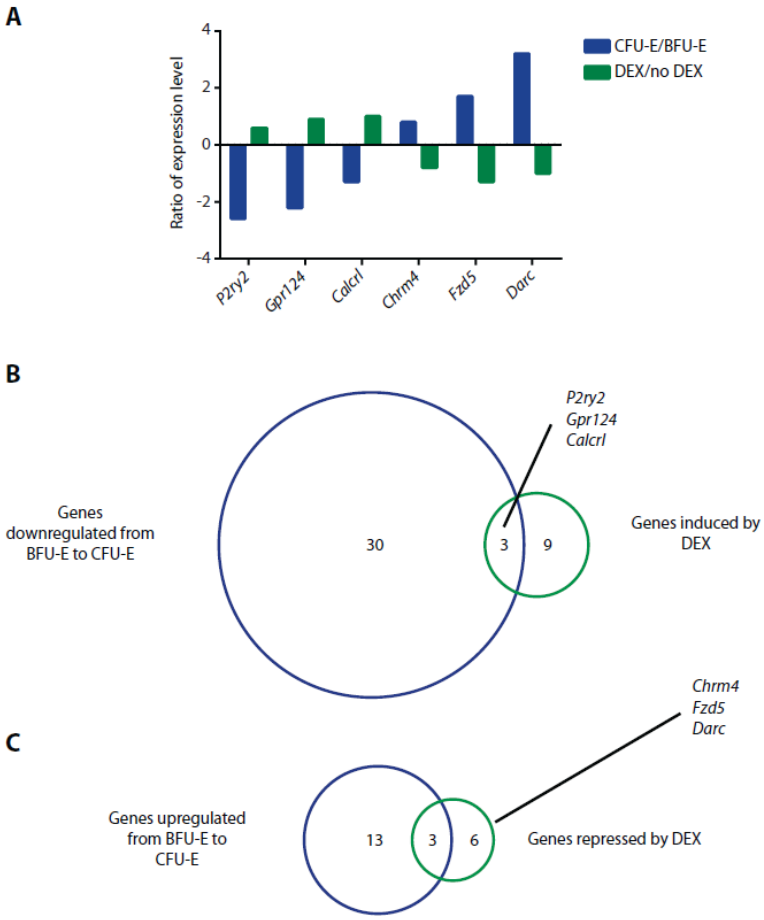


**Fig. S1. Gene expression analysis identifies six GPCRs with contrasting expression patterns between BFU-E differentiation and self-renewal.** (**A**) Blue columns represent ratios of the expression of each indicated gene at the CFU-E stage to its expression at the BFU-E stage. Highly purified murine BFU-Es were isolated as lin$^-$Ter119$^-$CD16/CD32$^-$Sca-1$^-$CD41$^-$c-Kit$^+$CD71/Cd24a$^{10\%low}$ population, and highly purified murine CFU-Es were isolated as lin$^-$Ter119$^-$CD16/CD32$^-$Sca-1$^-$CD41$^-$c-Kit$^+$CD71/Cd24a$^{20\%high}$ population from murine fetal liver as previously reported (*14*, *15*). Green columns represent ratios of the expression of each indicated gene in murine fetal liver BFU-Es cultured in the presence of dexamethasone (DEX) to their expression in murine fetal liver BFU-Es cultured in the absence of DEX. Gene expression results were analyzed from previous reports (*14*, *15*). (**B**) Schematic diagram shows genes that are downregulated from the BFU-E to the CFU-E stage of murine fetal liver and upregulated by DEX treatment. GPCRs were filtered by cutoffs with downregulation < 0.7 fold, and upregulation > 1.4 fold. (**C**) Schematic diagram shows genes that are upregulated from the BFU-E to the CFU-E stage of murine fetal liver and downregulated by DEX. GPCRs were filtered by cutoffs with downregulation < 0.7 fold, and upregulation > 1.4 fold.

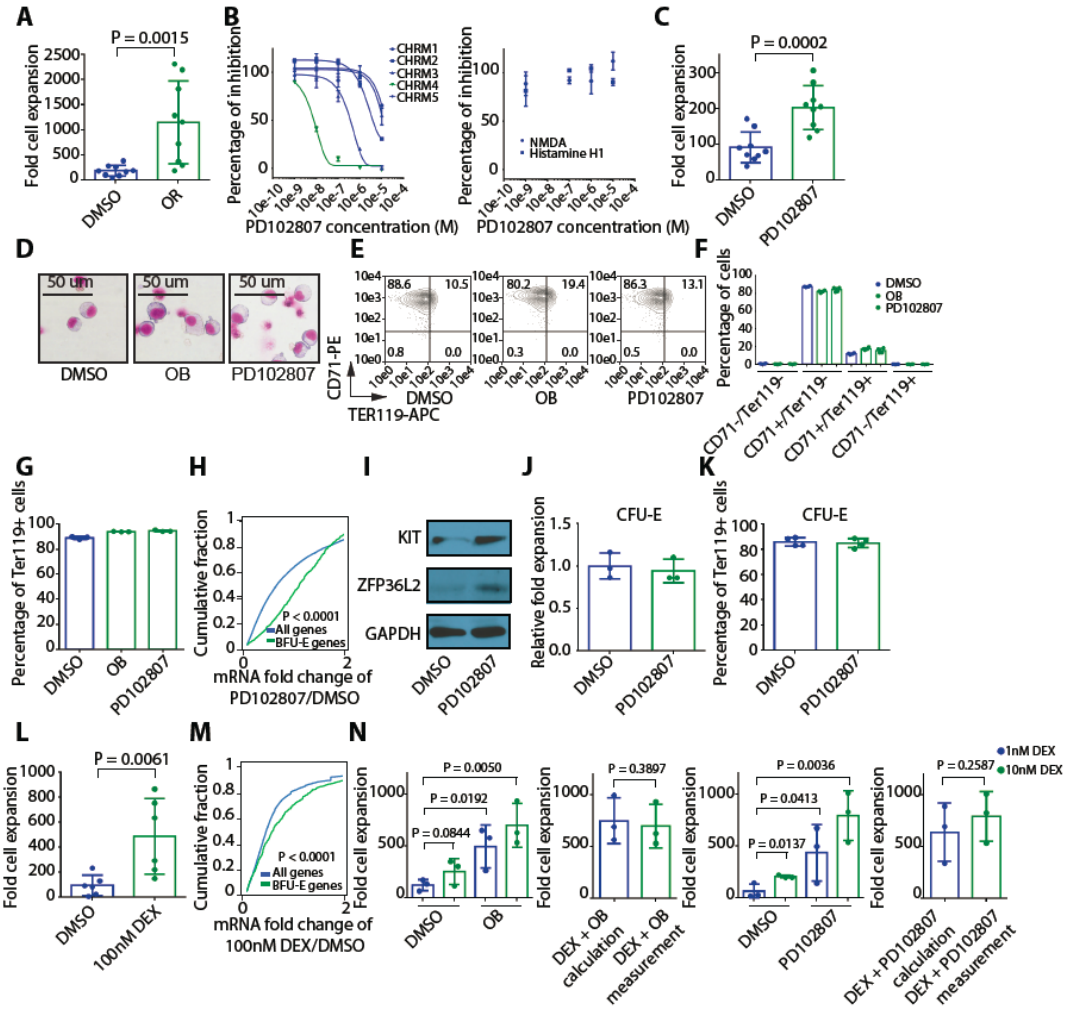


**Fig. S2. Muscarinic acetylcholine receptor antagonists increase erythropoiesis and BFU-E expansion in mouse BFU-E culture system.** (**A**) Murine fetal liver BFU-Es were cultured with or without 1 μM orphenadrine citrate (OR). Total numbers of cells in the culture system were counted on day 9. The mean and SD of total numbers of cells of 9 measurements from distinct samples are shown. *P* value was calculated using the one-tailed t-test. (**B**) Protein binding assay was performed for PD102807 on indicated receptors including CHRM1, CHRM2, CHRM3, CHRM4, and CHRM5. The mean and SD of 2 measurements from distinct samples are shown. Protein binding assay was performed for PD102807 on indicated receptors including NMDA and histamine H1 receptors. The mean and SD of 2 measurements from distinct samples are shown. The original data are in data file S3. (**C**) Murine fetal liver BFU-Es were cultured with or without 3 nM PD102807. Total numbers of cells in the culture system were counted on day 9. The mean and SD of total numbers of cells of 9 measurements from distinct samples are shown. *P* value was calculated using the one-tailed t-test. (**D**) Murine fetal liver BFU-Es were cultured with or without 100 μM OB or 3 nM PD102807. May-Grünwald Giemsa staining of day 9 cultured cells is shown. (**E**) Murine fetal liver BFU-Es were cultured with or without 100 μM OB or 3 nM PD102807. The representative flow cytometry of 4 measurements from distinct samples of CD71 and TER119 staining of day 6 cultured cells is shown. Flow cytometry control gating plots are in fig. S23. (**F**) The mean and SD of percentage of $CD71^-/TER119^-$ cells, $CD71^+/TER119^-$ cells,

$CD71^+/TER119^+$ cells, and $CD71^-/TER119^+$ cells in panel E of 4 measurements from distinct samples are shown. (**G**) Murine fetal liver BFU-Es were cultured with or without 100 μM OB or 3 nM PD102807. Cells were stained with anti-Ter119 antibody at the end of culture and analyzed with flow cytometry. The mean and SD of the percentage of $Ter119^+$ cells of 3 measurements from distinct samples are shown. (**H**) Murine fetal liver BFU-Es were cultured with DMSO or 3 nM PD102807, and RNA-Seq was performed on cultured cells. The x-axis represents the ratio of each gene's expression in BFU-Es cultured with PD102807 relative to BFU-Es cultured with DMSO. The y-axis represents the cumulative fraction and is plotted as a function of the relative expression. 'BFU-E genes' represents a group of 650 genes most dramatically downregulated during erythroid differentiation from the BFU–E to the CFU-E stage. 'All genes' represents all the genes expressed in BFU-E as reported previously (*15*). *P* value was calculated using the Kolmogorov-Smirnov test. (**I**) Murine fetal liver BFU-Es were cultured with DMSO or 3 nM PD102807, and western blot was performed on day 6 cultured cells to detect KIT and ZFP36L2. Unprocessed blots are in fig. S22. (**J**) Murine fetal liver CFU-Es were cultured with or without 3 nM PD102807, and cell numbers in the culture system were counted on day 3 of culture. The mean and SD of relative cell proliferation of 3 measurements from distinct samples are shown. (**K**) Murine fetal liver CFU-Es cultured with or without 3 nM PD102807 were stained with anti-Ter119 antibody on day 3 of culture and analyzed with flow cytometry. The mean and SD of the percentage of $Ter119^+$ cells of 4 measurements from distinct samples are shown. (**L**) Murine fetal liver BFU-Es were cultured with or without 100 nM dexamethasone (DEX). Total numbers of cells in the culture system were counted on day 9. The mean and SD of total numbers of cells of 6 measurements from distinct samples are shown. *P* value was calculated using the one-tailed t-test. (**M**) Murine fetal liver BFU-Es were cultured with DMSO or 100 nM DEX, and RNA-Seq was performed on cultured cells. The x-axis represents the ratio of each gene's expression in BFU-Es cultured with 100 nM DEX relative to BFU-Es cultured with DMSO. The y-axis represents the cumulative fraction and is plotted as a function of the relative expression. 'BFU-E genes' represents a group of 650 genes most dramatically downregulated during erythroid differentiation from the BFU–E to the CFU-E stage. 'All genes' represents all the genes expressed in BFU-E as reported previously (*15*). *P* value was calculated using the Kolmogorov-Smirnov test. (**N**) Murine fetal liver BFU-Es were cultured with or without 100 μM OB or 3 nM PD102807 in the presence of 1 nM or 10 nM of DEX. Total numbers of cells in the culture system were counted on day 9. The mean and SD of total numbers of cells of 3 measurements from distinct samples are shown. "DEX + OB calculation" represents the sum of total numbers of cells from sample treated with 10 nM DEX and sample treated with 100 μM OB. "DEX + OB measurement" represents the total number of cells from sample treated with 10 nM DEX and 100 μM OB. "DEX + PD102807 calculation" represents the sum of total numbers of cells from sample treated with 10 nM DEX and sample treated with 3 nM PD102807. "DEX + PD102807 measurement" represents the total number of cells from sample treated with 10 nM DEX and 3 nM PD102807. *P* values were calculated using the one-tailed t-test.

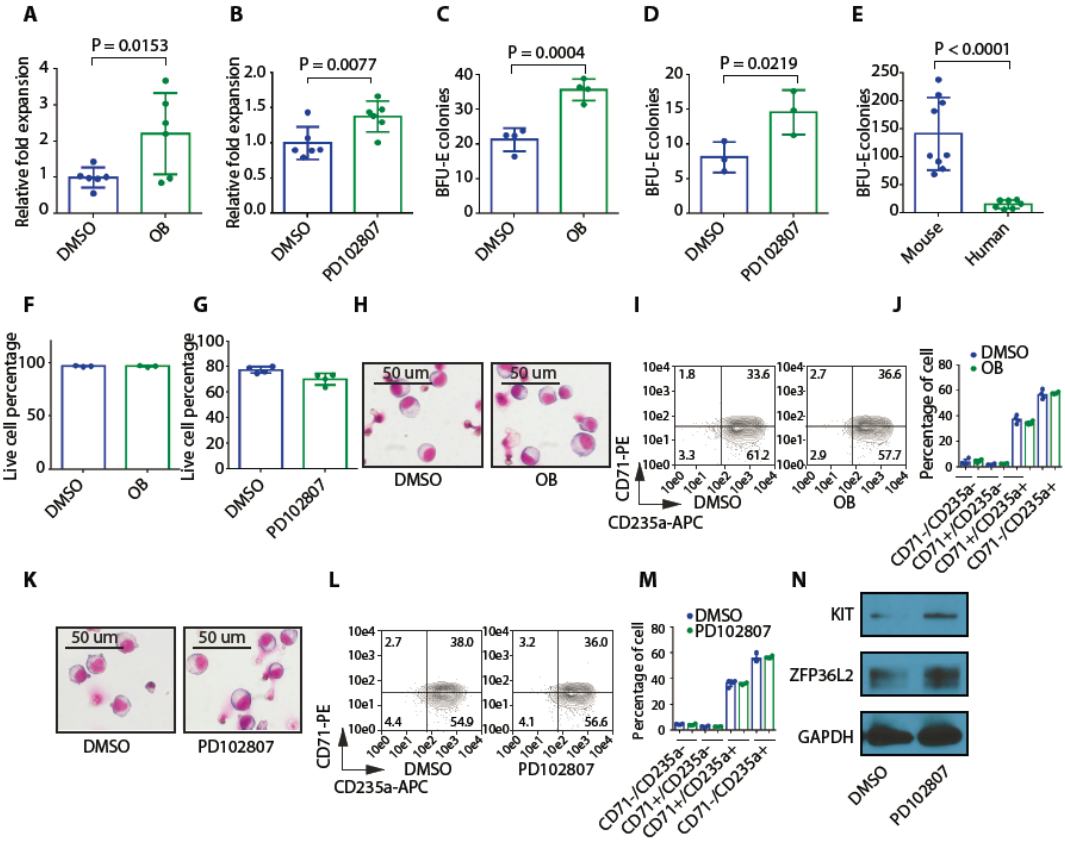


**Fig. S3. Muscarinic acetylcholine receptor antagonists induce erythroid expansion in erythroid differentiation system cultured human CD34$^+$ cells.** (**A**) Human CD34$^+$ cells were cultured in erythroid differentiation system with or without 200 μM OB. Total numbers of cells in the culture system were counted on day 22, and the mean and SD of relative fold cell expansion of 6 measurements from distinct samples are shown. (**B**) Human CD34$^+$ cells were cultured in erythroid differentiation system with or without 3 nM PD102807. Numbers of cells in the culture system were counted on day 16. The mean and SD of 6 measurements from distinct samples are shown. (**C**) Human CD34$^+$ cells were cultured and plated on methylcellulose medium for BFU-E colony formation assay. BFU-E colonies were counted on day 13 of colony formation assay, and the mean and SD of colony number of 4 measurements from distinct samples are shown. (**D**) Human CD34$^+$ cells were cultured and plated on methylcellulose medium for BFU-E colony formation assay. BFU-E colonies were counted on day 13 of colony formation assay, and the mean and SD of colony number of 3 measurements from distinct samples are shown. (**E**) Murine fetal liver BFU-Es were cultured and plated on methylcellulose medium. BFU-E colonies were counted on day 9 of colony formation assay, and the mean and SD of BFU-E colonies from 100 day 0 BFU-Es of 9 measurements from distinct samples are shown. Human CD34$^+$ cells were cultured and plated on methylcellulose medium for BFU-E colony formation assay. BFU-E colonies were counted on day 13 of colony formation assay, and the mean and SD of colony number from 100 day 0 CD34$^+$ cells of 7 measurements from distinct samples are shown. (**F**) Human CD34$^+$ cells were cultured in erythroid differentiation system with or without 200 μM OB. Percentages of live cells in the culture system were counted on day 12. The mean and SD of 3 measurements from distinct samples are shown. (**G**) Human CD34$^+$

cells were cultured in erythroid differentiation system with or without 3 nM PD102807. Percentages of live cells in the culture system were counted on day 9. The mean and SD of 4 measurements from distinct samples are shown. (**H**), Human $CD34^+$ cells were cultured in erythroid differentiation system with or without 200 μM OB. May-Grünwald Giemsa staining was performed on day 20. (**I**) Human $CD34^+$ cells were cultured in erythroid differentiation system with or without 200 μM OB. The representative flow cytometry of 4 measurements from distinct samples of CD71 and CD235a staining of day 21 cultured cells is shown. Flow cytometry control gating plots are in fig. S23. (**J**)., The mean and SD of $CD71^-/CD235a^-$ cells, $CD71^+/CD235a^-$ cells, $CD71^+/CD235a^+$ cells, and $CD71^-/CD235a^+$ cells analyzed as in panel I of 4 measurements from distinct samples are shown. (**K**) Human $CD34^+$ cells were cultured in erythroid differentiation system with or without 3 nM PD102807. May-Grünwald Giemsa staining was performed on day 22. (**L**) Human $CD34^+$ cells were cultured in erythroid differentiation system with or without 3 nM PD102807. The representative flow cytometry of 4 measurements from distinct samples of CD71 and CD235a staining of day 21 cultured cells is shown. Flow cytometry control gating plots are in fig. S23. (**M**) The mean and SD of $CD71^-/CD235a^-$ cells, $CD71^+/CD235a^-$ cells, $CD71^+/CD235a^+$ cells, and $CD71^-/CD235a^+$ cells analyzed as in panel L of 4 measurements from distinct samples are shown. (**N**) Human $CD34^+$ cells were cultured in erythroid differentiation system with DMSO or 3 nM PD102807, and western blot was performed on day 6 cultured cells to detect KIT and ZFP36L2. Unprocessed blots are in fig. S22. All *P* values were calculated using the one-tailed t-test.

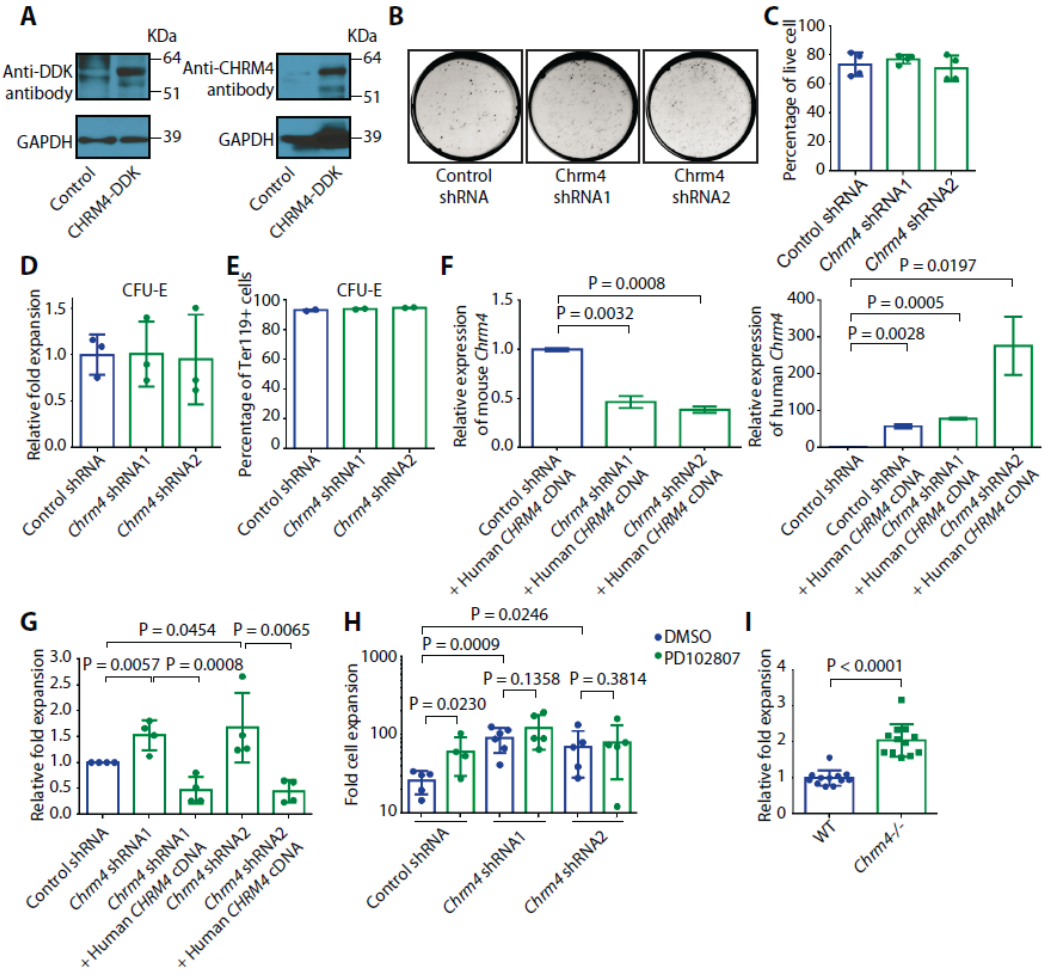


**Fig. S4. CHRM4 regulates erythropoiesis and BFU-E expansion in mouse BFU-E culture system.** (**A**) Plasmids encoding C-terminus DDK-tagged CHRM4 or control vector were transfected into 293T cells. Western blots with anti-DDK or anti-CHRM4 antibodies were performed to measure the expression of DDK-tagged CHRM4. Unprocessed blots are in fig. S22. (**B**) Murine fetal liver BFU-Es were infected with either control virus or virus encoding shRNA targeting *Chrm4*. $GFP^+$ cells were sorted and seeded for BFU-E colony formation assay. The representative results of 4 measurements from distinct samples of BFU-E colonies from day 9 of colony formation assay are shown. (**C**) Murine fetal liver BFU-Es were infected with either control virus or viruses encoding shRNA targeting *Chrm4*. Live cell percentages were measured on day 6 cultured cells, and the mean and SD of 4 measurements from distinct samples are shown. (**D**) Murine fetal liver CFU-Es were infected with either control virus or viruses encoding shRNA targeting *Chrm4*, and cell numbers in the culture system were counted on day 3 of culture. The mean and SD of relative cell proliferation of 3 measurements from distinct samples are shown. (**E**) Murine fetal liver CFU-Es infected with either control virus or viruses encoding shRNA targeting *Chrm4* were stained with anti-Ter119 antibody on day 3 of culture and analyzed with flow cytometry. The mean and SD of the percentage of $Ter119^+$ cells of 2 measurements from distinct samples are shown. (**F**) Expression of mouse *Chrm4* (left panel) and human *CHRM4* (right panel) in murine fetal liver BFU-Es in the presence or absence of anti-

mouse *Chrm4* shRNAs and human *CHRM4* cDNA were measured by RT-PCR and normalized to *GAPDH*. The mean and SD of 3 measurements from distinct samples are shown. The original data are in data file S3. (**G**) Murine fetal liver BFU-Es were infected with either control virus or virus encoding shRNA targeting *Chrm4* together with control virus or virus encoding human CHRM4 cDNA. The numbers of puromycin-resistant and $GFP^+$ cells in the culture system were counted. The mean and SD of 4 measurements from distinct samples are shown. (**H**) Murine fetal liver BFU-Es were infected with either control virus or virus encoding shRNA targeting *Chrm4* together with DMSO or 3 nM PD102807. The numbers of $GFP^+$ cells in the culture system were counted on day 9 of culture. The mean and SD of 5 measurements from distinct samples are shown. (**I**) Murine fetal liver BFU-Es were isolated from wild type mice or *Chrm4*$^{-/-}$ mice. The numbers of cells in the culture system were counted. The mean and SD of 12 measurements from distinct samples are shown. All *P* values were calculated using the one-tailed t-test.

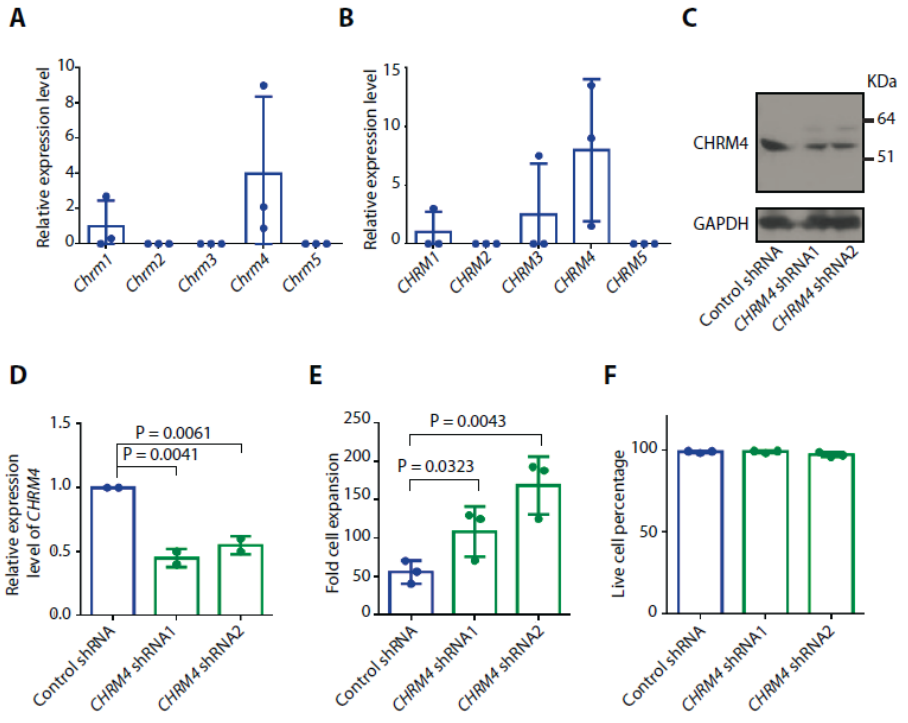


**Fig. S5. CHRM4 regulates erythroid expansion in erythroid differentiation system cultured human CD34$^+$ cells.** (**A**) The relative expression of mouse muscarinic acetylcholine receptor family members, *Chrm1*, *Chrm2*, *Chrm3*, *Chrm4*, and *Chrm5*, in erythroid progenitors are shown. The mean and SD of 3 measurements from distinct samples analyzed from previously published database are shown (*49*). (**B**) The relative expression of human muscarinic acetylcholine receptor family members, *CHRM1*, *CHRM2*, *CHRM3*, *CHRM4*, and *CHRM5*, in erythroid progenitors are shown. The mean and SD of 3 measurements from distinct samples analyzed from previously published database are shown (*49*). (**C**) The knockdown efficiency of human *CHRM4* shRNAs is shown using western blot experiment. Unprocessed blots are in fig. S22. (**D**) The mean and SD of quantification of expression of CHRM4 relative to GAPDH as in panel C of 2 measurements from distinct samples are shown. (**E**) Human CD34$^+$ cells were infected with indicated viral shRNAs and cultured in erythroid differentiation system. Numbers of cells in the culture system were counted on day 12. The mean and SD of 3 measurements from distinct samples are shown. (**F**) Human CD34$^+$ cells were infected with indicated viral shRNAs and cultured in erythroid differentiation system. Percentages of live cells in the culture system were counted on day 20. The mean and SD of 3 measurements from distinct samples are shown. All *P* values were calculated using the one-tailed t-test.

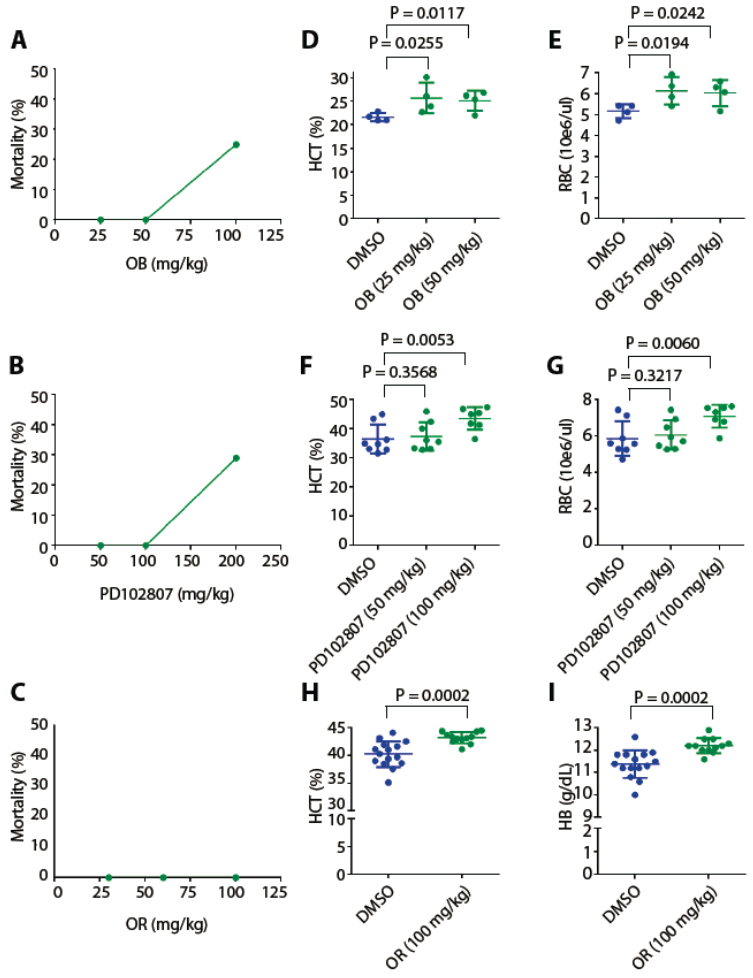


**Fig. S6. Maximal tolerance and pharmacodynamics studies identify maximal tolerance and effective doses of muscarinic acetylcholine receptor antagonists.** (**A**) C57bl/6 mice were intraperitoneally treated with 25, 50, or 100 mg/kg OB daily (n = 12, 4, and 4 for 25 mg/kg, 50 mg/kg, and 100 mg/kg OB groups, respectively). The percentage of mouse mortality within 7 days of OB treatment at each dose is shown. (**B**) C57bl/6 mice were orally treated with 50, 100, or 200 mg/kg PD102807 daily (n = 7, 7, and 7 for 50 mg/kg, 100 mg/kg, and 200 mg/kg PD102807 groups, respectively). The percentage of mouse mortality within 7 days of PD102807 treatment at each dose is shown. (**C**) C57bl/6 mice were intraperitoneally treated with 30, 60, or 100 mg/kg OR daily (n = 10, 7, and 6 for 30 mg/kg, 60 mg/kg, and 100 mg/kg OR groups, respectively). The percentage of mouse mortality within 7 days of OR treatment at each dose is shown. (**D**) Mice were intraperitoneally treated with DMSO or 25 or 50 mg/kg OB daily. Anemia was induced with 60 mg/kg phenylhydrazine (PHZ), and CBC was performed 3 days after PHZ injection. The mean and SD of HCT are shown (n = 4 per group). (**E**) The mean and SD of RBC counts are shown (n = 4 per group). (**F**) Mice were orally treated with DMSO or 50 or 100 mg/kg PD102807 daily. Anemia was induced with 60 mg/kg PHZ, and CBC was performed 3 days after PHZ injection. The mean and SD of HCT are shown (n = 8, 8, and 7 for DMSO, 50 mg/kg, and 100 mg/kg PD102807, groups respectively). (**G**) The mean and SD of RBC counts are shown (n = 8, 8, and 7 for DMSO, 50 mg/kg, and 100 mg/kg PD102807 groups,

respectively). 8-week-old female mice were used. Each dot represents one mouse. (**H**) *Mx1-Cre Srsf2*$^{P95H/WT}$ MDS mice were intraperitoneally treated with DMSO or 100 mg/kg OR daily. CBC was performed on day 18. The mean and SD of HCT are shown (n = 15 and 12 for DMSO and 100 mg/kg OR groups, respectively). (**I**) The mean and SD of Hb are shown (n = 15 and 12 for DMSO and 100 mg/kg OR groups, respectively). All *P* values were calculated using the one-tailed t-test.

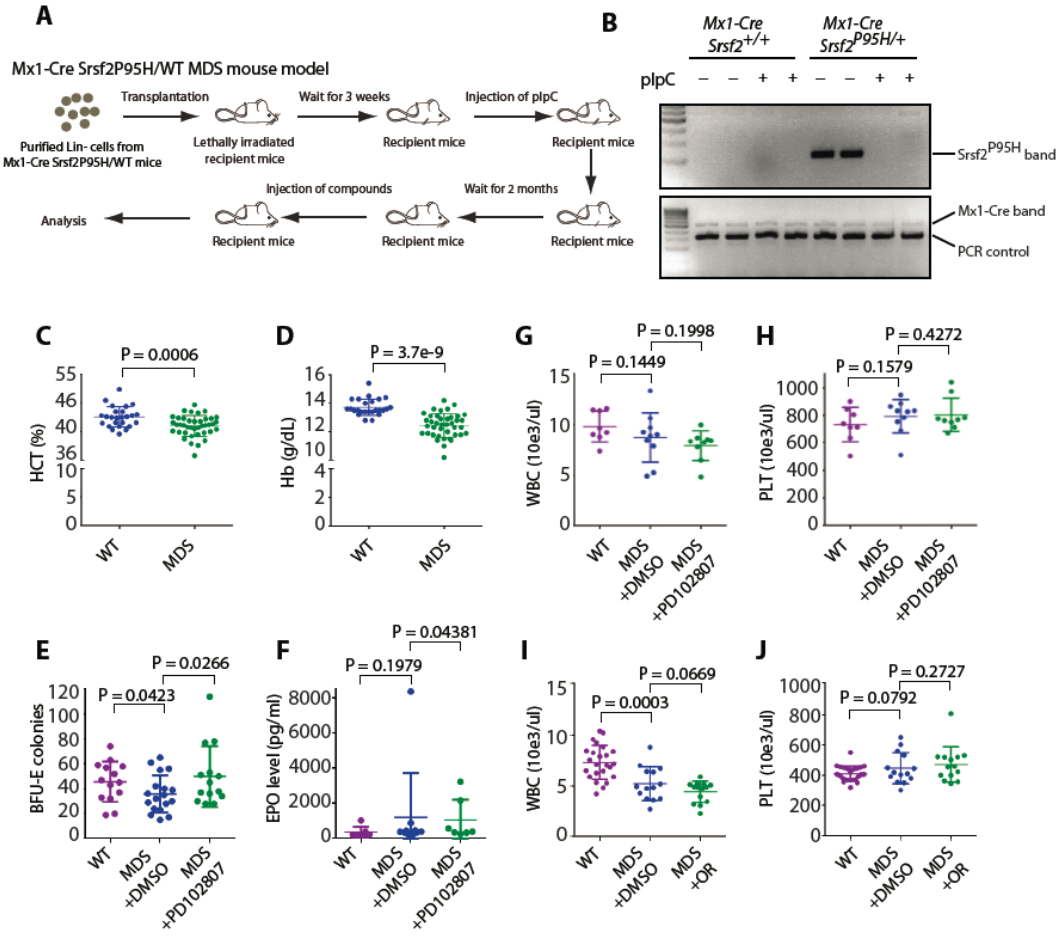


**Fig. S7. Muscarinic acetylcholine receptor antagonists do not influence white blood cell and platelet production in the *Mx1-Cre Srsf2*$^{P95H/WT}$ MDS mouse model.** (**A**) Schematic diagram shows the *Mx1-Cre Srsf2*$^{P95H/WT}$ MDS mouse model. (**B**) PCR from mononuclear cells from the peripheral blood of *Mx1-Cre Srsf2*$^{WT/WT}$ and *Mx1-Cre Srsf2*$^{P95H/WT}$ mice before and after pIpC treatment. The absence of a PCR product represents successful recombination after pIpC treatment. (**C**) The mean and SD of HCT values of *Mx1-Cre Srsf2*$^{WT/WT}$ control mice and *Mx1-Cre Srsf2*$^{P95H/WT}$ MDS mice before OB, OR, or PD102807 injection are shown (n = 25 and 40 for WT and MDS groups, respectively), (**D**) The mean and SD of Hb values of *Mx1-Cre Srsf2* $^{WT/WT}$ control mice and *Mx1-Cre Srsf2* $^{P95H/WT}$ MDS mice before OB, OR, or PD102807 injection are shown (n = 25 and 40 for WT and MDS groups, respectively). (**E**) *Mx1-Cre Srsf2* $^{P95H/WT}$ MDS mice were orally treated with DMSO or 100 mg/kg PD102807 daily. Spleens were dissected for BFU-E colony formation assay, and the mean and SD of numbers of BFU-E colonies are shown (n = 14, 18, and 14 for WT, MDS+DMSO, and MDS+PD102807 groups, respectively). (**F**) The mean and SD of plasma EPO concentrations are shown (n = 7, 10, and 7 for WT, MDS+DMSO, and MDS+PD102807 groups, respectively). (**G**) *Mx1-Cre Srsf2* $^{P95H/WT}$ MDS mice were orally treated with DMSO or 100 mg/kg PD102807 daily. CBC was performed on day 15. The mean and SD of WBC counts are shown (n = 8, 10, and 9 for WT, MDS+DMSO, and MDS+PD102807 groups, respectively). (**H**) The mean and SD of PLT counts are shown (n = 8, 10, and 9 for WT, MDS+DMSO, and MDS+PD102807 groups, respectively). (**I**) *Mx1-Cre Srsf2*

$^{P95H/WT}$ MDS mice were injected with DMSO or 100 mg/kg OR daily. CBC was performed on day 45. The mean and SD of WBC counts are shown (n = 21, 13, and 13 for WT, MDS+DMSO, and MDS+OR groups, respectively). (**J**) The mean and SD of PLT counts are shown (n = 21, 13, and 13 for WT, MDS+DMSO, and MDS+OR groups, respectively). 8-week-old female mice were used. Each dot represents one mouse. All *P* values were calculated using the one-tailed t-test.

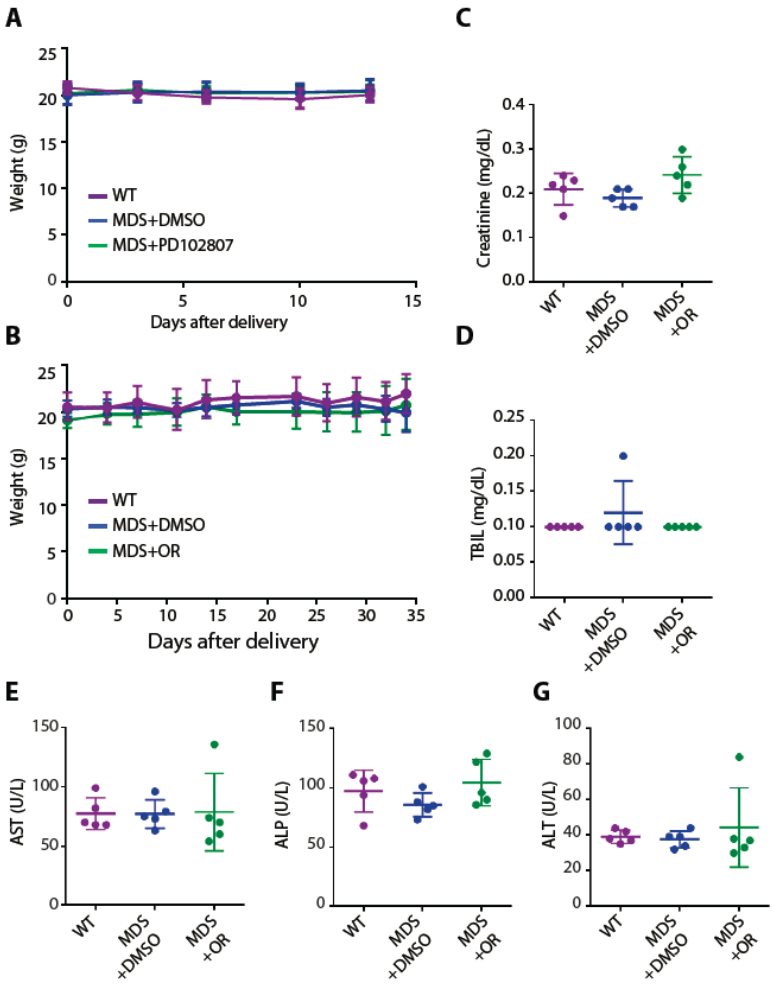


**Fig. S8. Muscarinic acetylcholine receptor antagonists exhibit well-tolerated safety profile in the *Mx1-Cre Srsf2*$^{P95H/WT}$ MDS mouse model.** (**A**) *Mx1-Cre Srsf2* $^{P95H/WT}$ MDS mice were orally treated with DMSO or 100 mg/kg PD102807 daily. The mean and SD of mouse weights during treatment are shown (n = 8, 10, and 10 for WT, MDS+DMSO, and MDS+PD102807 groups, respectively), The original data are in data file S3. (**B**) *Mx1-Cre Srsf2*$^{P95H/WT}$ MDS mice were injected with DMSO or 100 mg/kg OR daily for 5 weeks. Mouse weights during treatment are shown (n = 8, 7 and 7 for WT, MDS+DMSO, and MDS+OR groups, respectively). The original data are in data file S3. (**C**) The mean and SD of creatinine values are shown (n = 5 per group). (**D**) The mean and SD of total bilirubin (TBIL) values are shown (n = 5 per group). (**E**) The mean and SD of aspartate transaminase (AST) values are shown (n = 5 per group). (**F**) The mean and SD of alkaline phosphatase (ALP) values are shown (n = 5 per group). (**G**), The mean and SD of alanine transaminase (ALT) values are shown (n = 5 per group). 8-week-old female mice were used. Each dot represents one mouse.

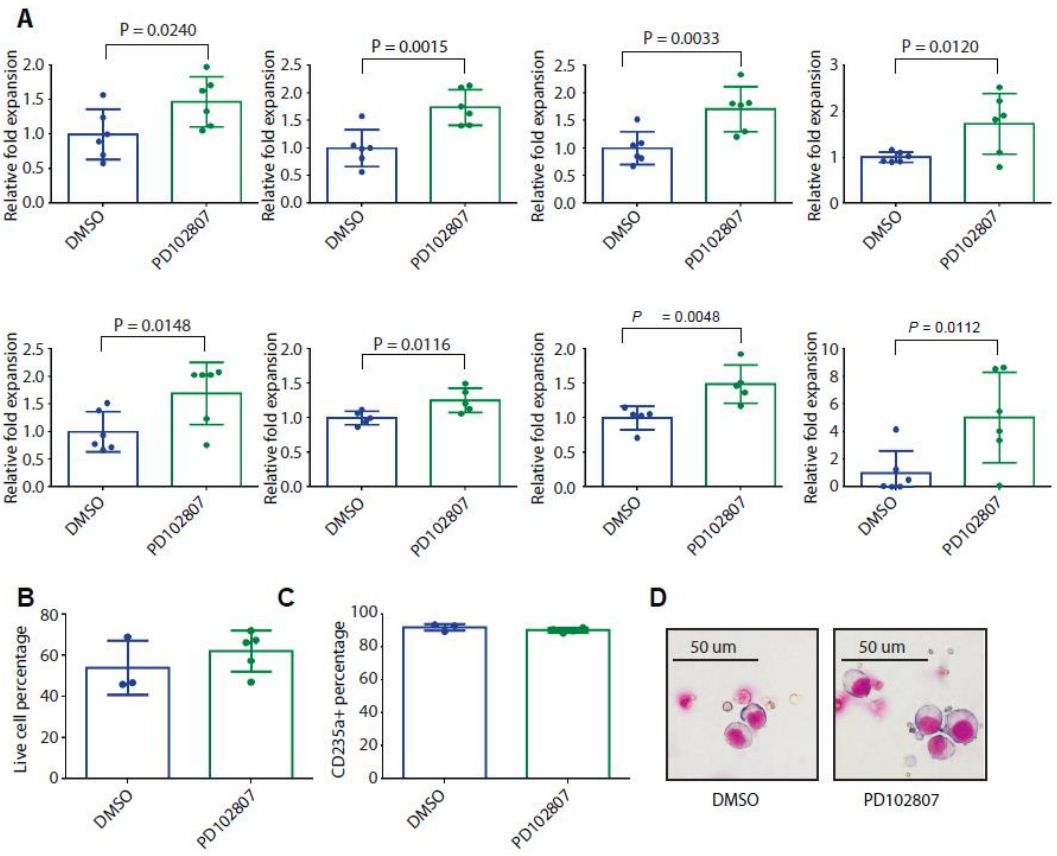


**Fig. S9. Muscarinic acetylcholine receptor antagonist PD102807 promotes expansion of human CD34$^+$ cells isolated from patients with MDS in erythroid differentiation culture system.** (**A**) CD34$^+$ cells isolated from 8 MDS patients were cultured in erythroid differentiation culture system in the presence of DMSO or 3 nM PD102807. Cell numbers in the culture system were counted on day 9, and the mean and SD of 5 or 6 measurements per patient from distinct samples are shown. (**B**) Human MDS CD34$^+$ cells were cultured in erythroid differentiation culture system in the presence of DMSO or 3 nM PD102807. Live cell percentages were counted on day 17, and the mean and SD of 3 measurements from distinct samples are shown. (**C**) Human MDS CD34$^+$ cells were cultured in erythroid differentiation culture system in the presence of DMSO or 3 nM PD102807. CD235a positive cell percentages were counted on day 21, and the mean and SD of 3 measurements from distinct samples are shown. (**D**) May-Grünwald Giemsa staining was performed on day 22, and a representative patient sample from fig. S9A is shown. All *P* values were calculated using the one-tailed t-test.

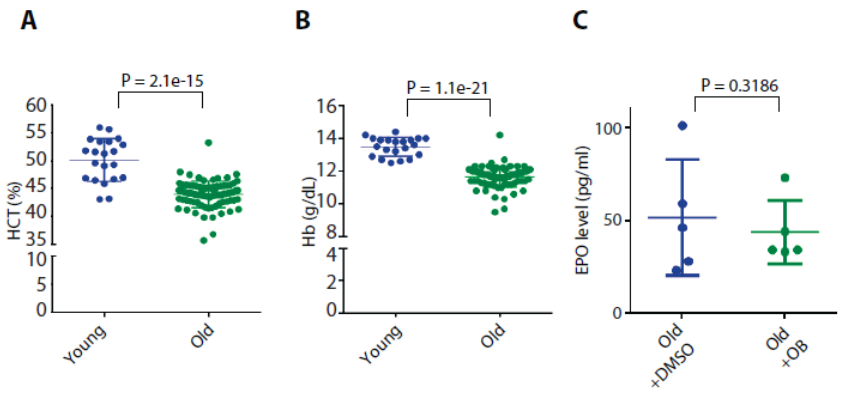


**Fig. S10. Muscarinic acetylcholine receptor antagonists exhibit no influence on EPO concentration in an aging mouse model.** (**A**) The mean and SD of HCT of control young mice (6- to 8-week-old male and female mice) and aged mice (18- to 21-month-old male and female mice) before OB or PD102807 injection are shown (n = 21 and 84 for young and old groups, respectively). (**B**) The mean and SD of Hb of control young mice and aged mice before OB and PD102807 injection are shown (n = 21 and 83 for young and old groups, respectively). (**C**) Aged mice were injected with DMSO or 25 mg/kg OB daily. The mean and SD of plasma EPO concentrations are shown (n = 5 per group). Each dot represents one mouse. All *P* values were calculated using the one-tailed t-test.

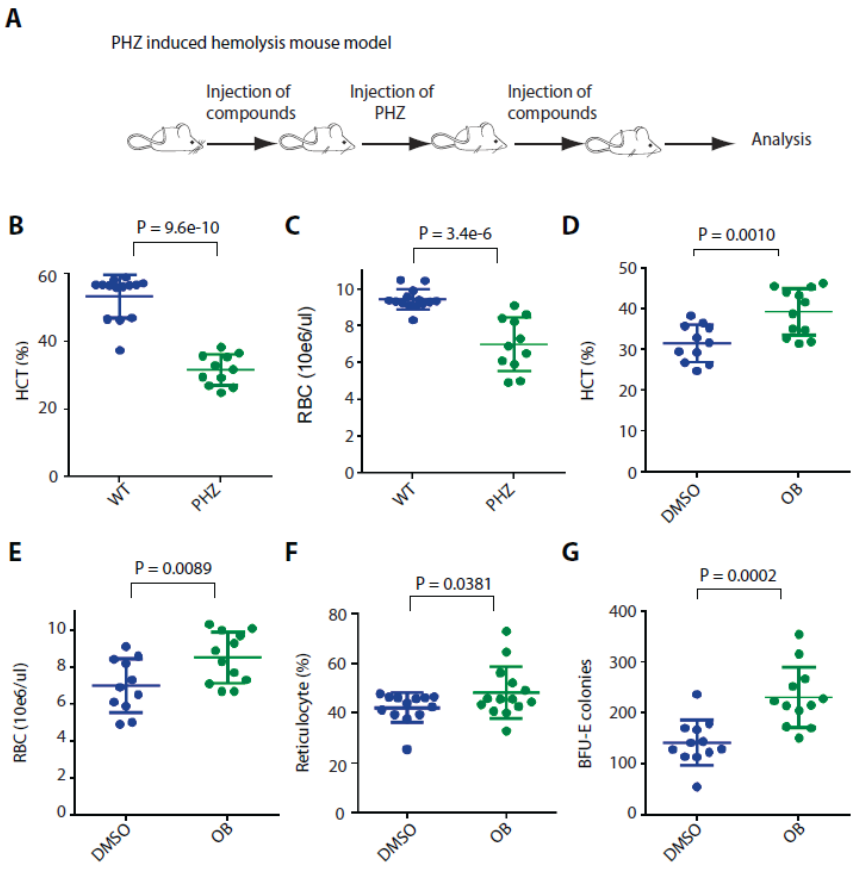


**Fig. S11. Muscarinic acetylcholine receptor antagonists correct anemia in a mouse model of acute hemolysis.** (**A**) Schematic diagram shows the PHZ-induced acute hemolysis mouse model. According to a previously established hemolytic anemia mouse model (*19*), mice were treated with DMSO, 25 mg/kg OB, or 100 mg/kg PD102807 daily for 3 days (day -3 to -1) before PHZ injection. Anemia was induced with 60 mg/kg PHZ on day 0. Mice were treated with DMSO, 25 mg/kg OB, or 100 mg/kg PD102807 from day 0 to 2, and CBC was performed on day 3. (**B**) The mean and SD of hematocrit (HCT) values of control mice and mice after PHZ injection are shown (n = 14 and 11 for WT and PHZ groups, respectively). (**C**) The mean and SD of red blood cell (RBC) values of control mice and mice after PHZ injection are shown (n = 14 and 11 for WT and PHZ groups, respectively). (**D**) Mice were injected with DMSO or 25 mg/kg OB daily. Anemia was induced with PHZ, and CBC was performed 3 days after PHZ injection. The mean and SD of HCT are shown (n = 11 and 12 for DMSO and OB groups, respectively). (**E**) The mean and SD of RBC counts are shown (n = 11 and 12 for DMSO and OB groups, respectively). (**F**) The mean and SD of reticulocyte counts are shown (n = 13 and 14 for DMSO and OB groups, respectively). (**G**) Spleens were dissected for BFU-E colony assay. The mean and SD of BFU-E colony numbers are shown (n = 12 per group). 8- to 10-week-old female mice were used. Each dot represents one mouse. All *P* values were calculated using the one-tailed t-test.

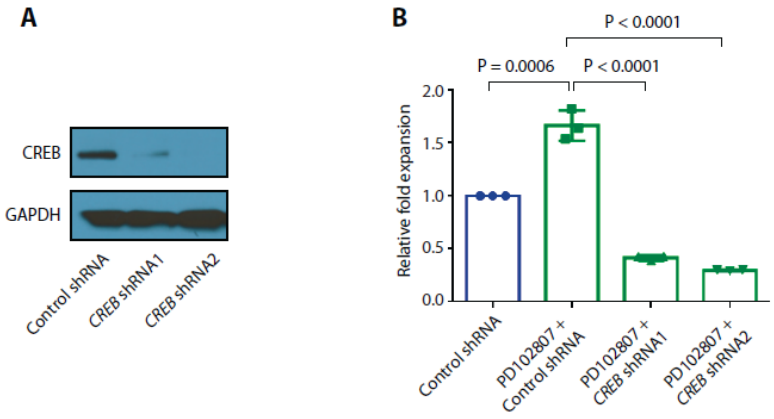


**Fig. S12. CREB is required for muscarinic acetylcholine receptor antagonist-induced expansion in erythroid-cultured human CD34$^+$ cells.** (**A**) The knockdown efficiency of human *CREB* shRNAs is shown using western blots. Unprocessed blots are in fig. S22. (**B**) Human CD34$^+$ cells were infected with indicated viral shRNAs and cultured in erythroid differentiation system together with DMSO or 3 nM PD102807. Numbers of cells in the culture system were counted on day 12. The mean and SD of 3 measurements from distinct samples are shown. *P* values were calculated using the one-tailed t-test.

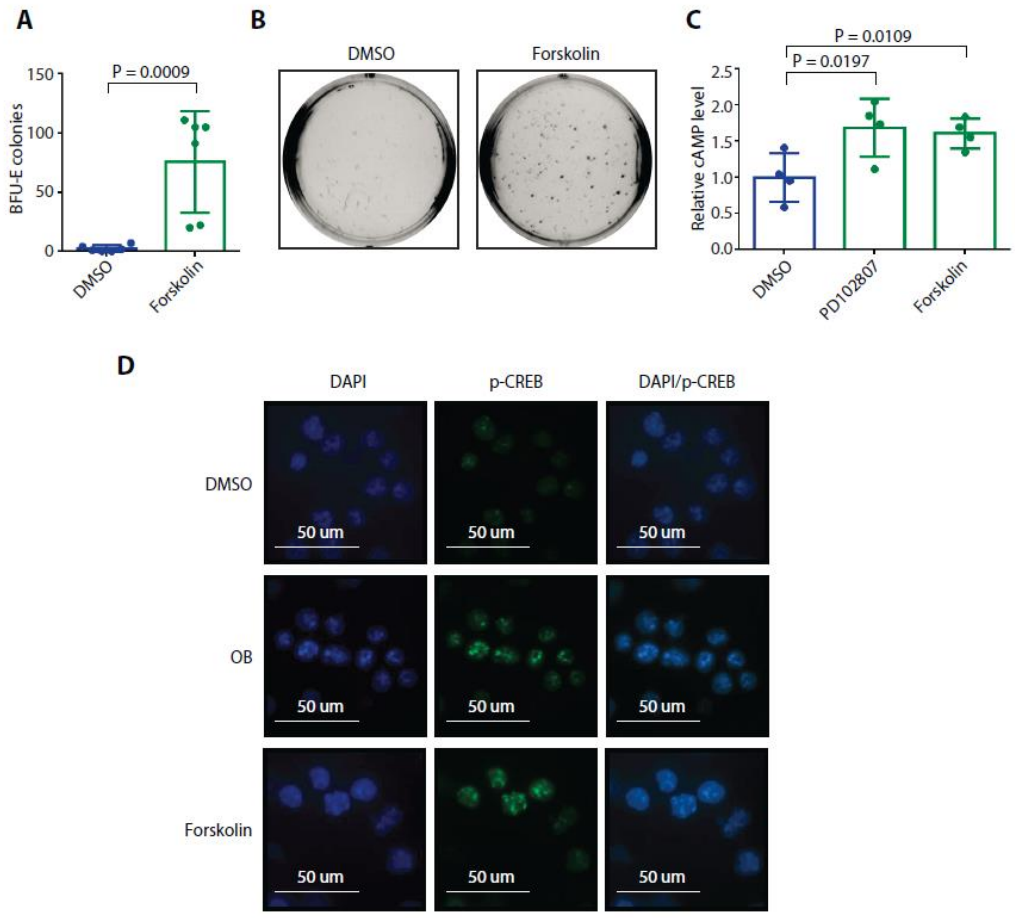


**Fig. S13. Muscarinic acetylcholine receptor antagonist increases cAMP and phosphorylation of CREB in BFU-E.** (**A**) Murine fetal liver BFU-Es were cultured with DMSO or 100 μM of forskolin and plated on methylcellulose medium. BFU-E colonies were counted on day 9 of colony formation assay, and the mean and SD of 6 measurements from distinct samples are shown. (**B**) The representative results of 6 measurements from distinct samples are shown. (**C**) Murine fetal liver BFU-Es were cultured with DMSO, 3 nM of PD102807, or 10 μM of forskolin for 45 min. cAMP concentrations were measured, and the mean and SD of 4 measurements from distinct samples are shown. (**D**), Murine fetal liver BFU-Es were cultured with DMSO, 100 μM of OB, or 100 μM of forskolin. Immunofluorescence images corresponding to DAPI, p-CREB, and the overlaps are shown. All *P* values were calculated using the one-tailed t-test.

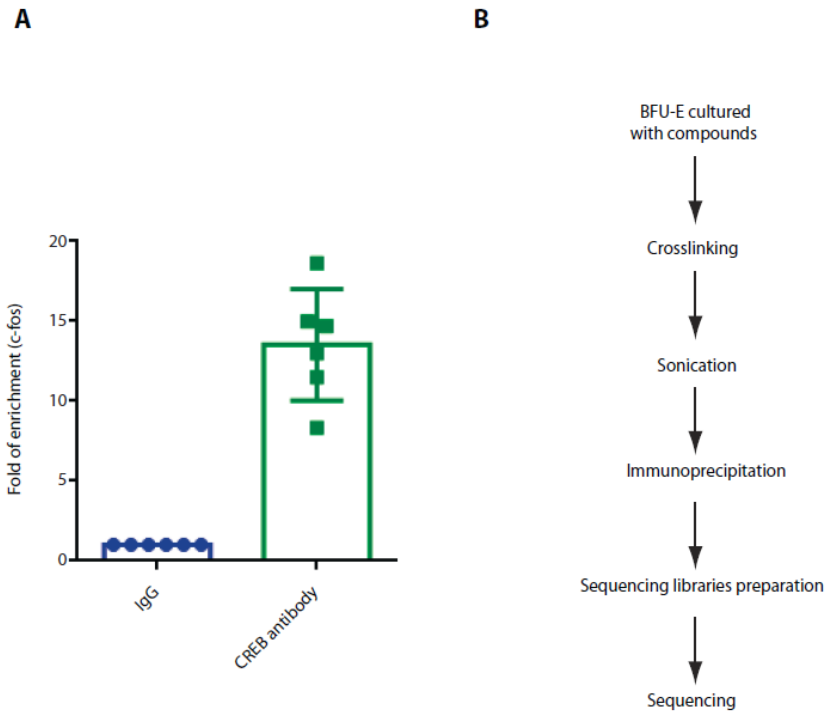


**Fig. S14. ChIP-PCR validates CREB antibody.** (**A**) Control IgG or CREB antibody was used for chromatin immunoprecipitation in 293 cells followed by RT-PCR analysis with a PCR primer for *c-Fos*. The mean and SD of 6 measurements from distinct samples are shown. (**B**) Schematic diagram shows the ChIP-Seq procedure.

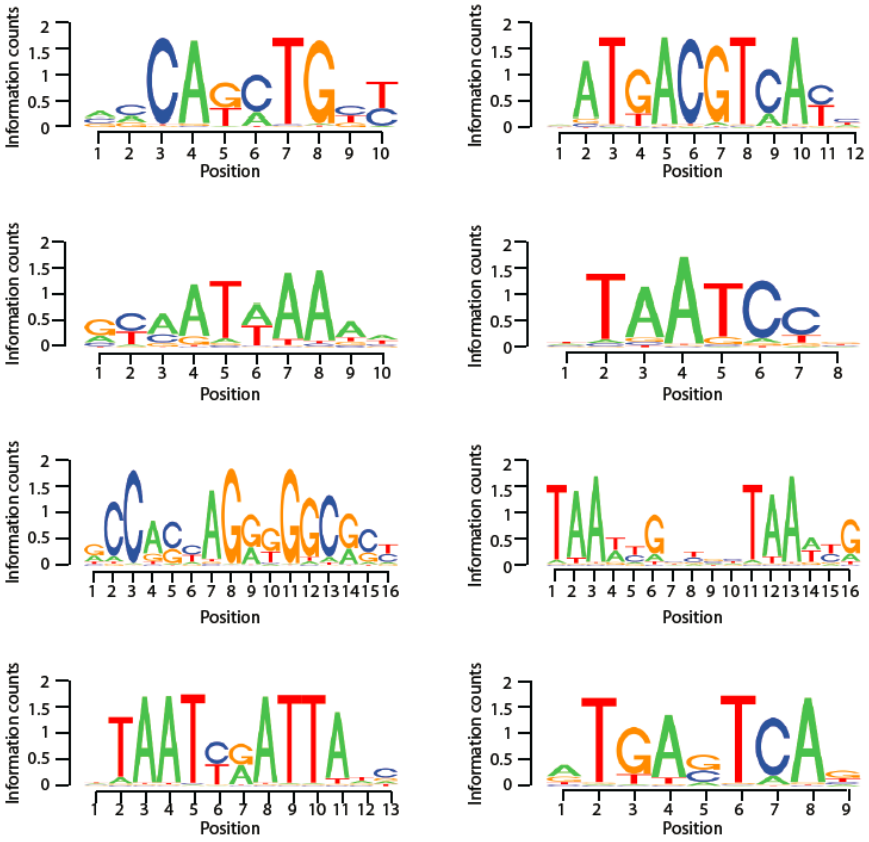


**Fig. S15. CREB-binding motifs are identified in BFU-E.** Murine fetal liver BFU-Es were cultured with DMSO or 100 μM of oxyphenonium bromide, and RNA-Seq was performed for cultured cells. RNA-Seq result and CREB ChIP-Seq result were combined for BETA analysis (*46*). CREB binding motifs for upregulated targets versus non-targets identified from BETA analysis are shown.

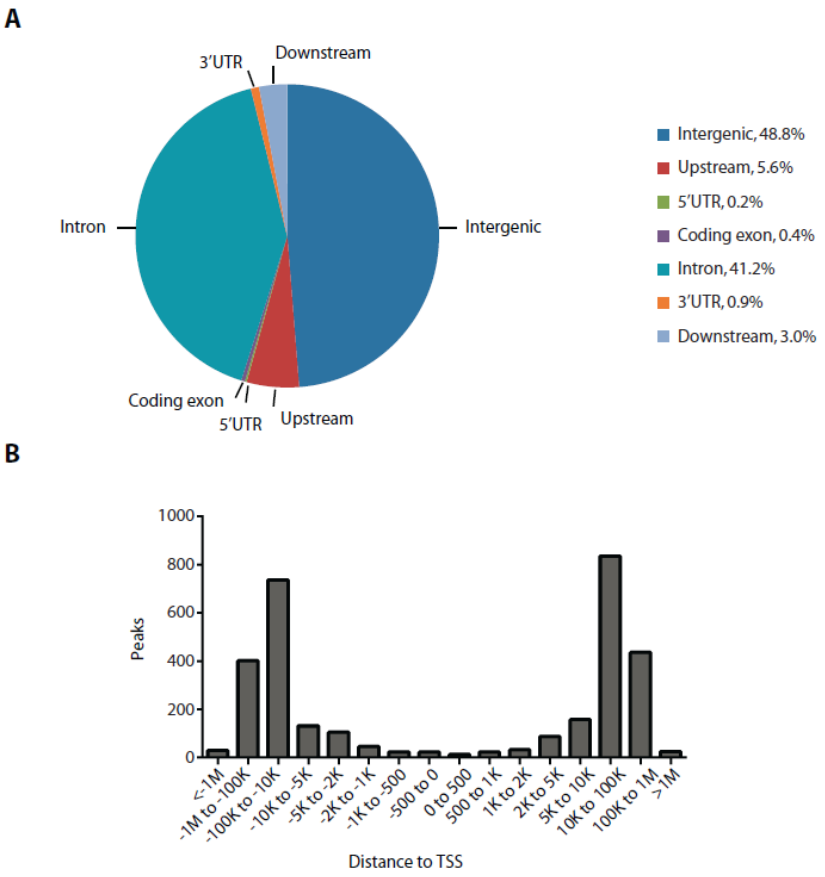


**Fig. S16. Genomic distributions of CREB binding sites are identified in BFU-E.** (**A**) Schematic diagram shows the genomic distribution of CREB binding sites. (**B**) Schematic diagram shows the distance from CREB ChIP-Seq peaks to the transcription start site (TSS).

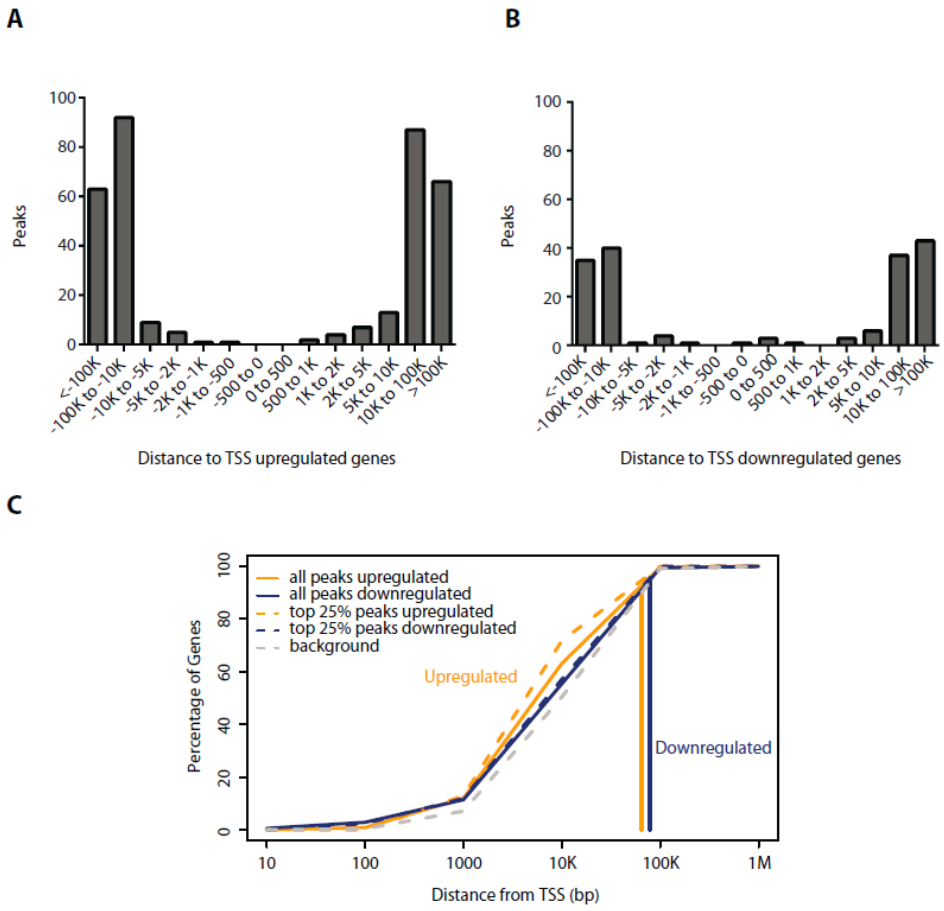


**Fig. S17. CREB target genes up-regulated and down-regulated by oxyphenonium bromide exhibit no binding preference.** (**A**) Schematic diagram shows the distance from CREB ChIP-Seq peaks to TSS for genes upregulated by 100 μM OB in murine fetal liver BFU-E. (**B**) Schematic diagram shows the distance from CREB ChIP-Seq peaks to TSS for genes downregulated by 100 μM OB in murine fetal liver BFU-E. (**C**) CREB binding sites were identified in BFU-Es using ChIP-Seq. The x-axis represents the distance from each CREB ChIP-Seq peak to TSS. The y-axis represents the percentage of genes and is plotted as a function of the distance to TSS (x axis) for each of the indicated CREB ChIP-Seq peak groups. The vertical lines represent median distance to the nearest binding site.

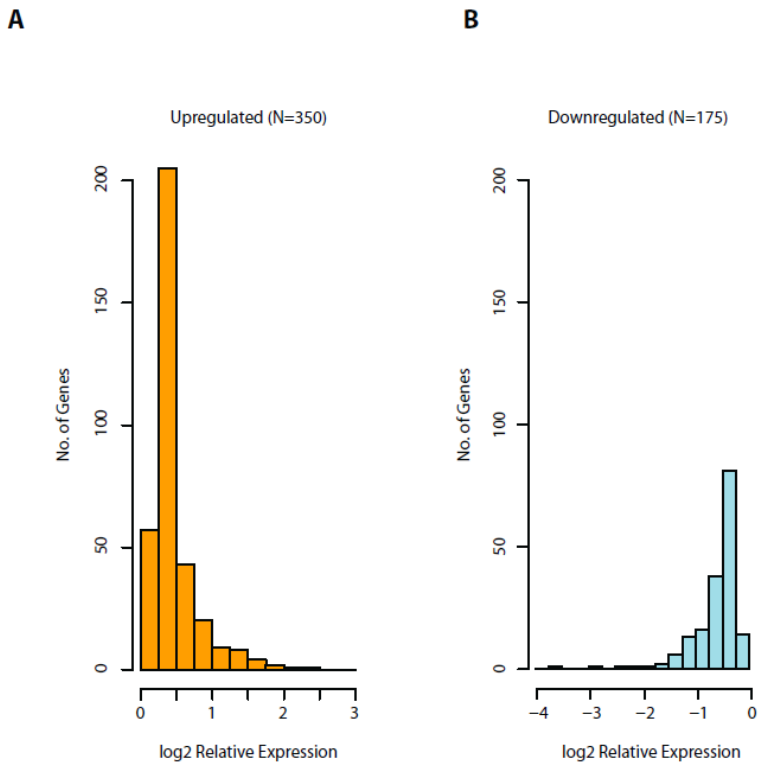


**Fig. S18. Numbers and expression changes of genes up-regulated or down-regulated by oxyphenonium bromide are identified.** (**A**) Schematic diagram shows numbers and expression changes of genes upregulated by 100 μM OB in murine fetal liver BFU-E. The x-axis represents ratios of the relative expression of genes in murine fetal liver BFU-Es cultured in the presence of 100 μM OB to their expression in murine fetal liver BFU-Es cultured in the presence of DMSO. The y-axis represents the number of genes for each of the indicated relative expression levels. (**B**) Schematic diagram shows numbers and expression changes of genes downregulated by 100 μM OB in murine fetal liver BFU-E. The x-axis represents ratios of the relative expression of genes in murine fetal liver BFU-Es cultured in the presence of 100 μM OB to their expression in murine fetal liver BFU-Es cultured in the presence of DMSO. The y-axis represents the number of genes for each of the indicated relative expression levels.

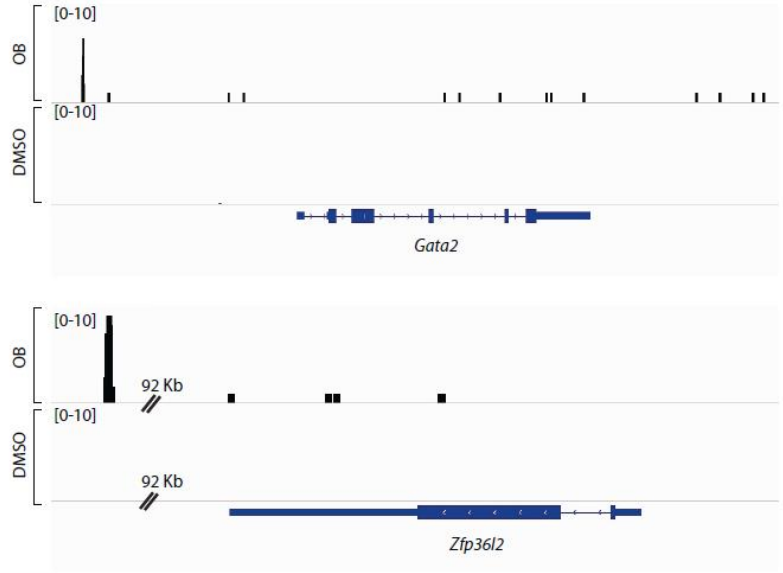


**Fig. S19. CREB binds to genomic loci near genes important for the maintenance of BFU-E progenitor status.** Anti-CREB ChIP-Seq was performed on BFU-Es after culture with either DMSO or 100 μM OB. Schematic diagram shows ChIP-Seq binding sites of CREB near *Gata2* and *Zfp36l2*.

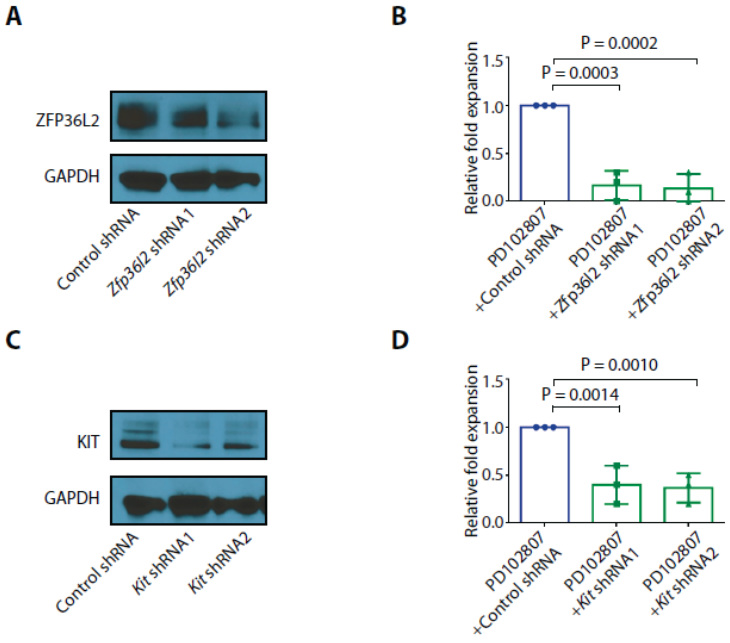


**Fig. S20. ZFP36L2 and KIT function downstream of CHRM4 to regulate mouse BFU-E expansion.** (**A**) The knockdown efficiency of mouse *Zfp36l2* shRNAs is shown using western blots. Unprocessed blots are in fig. S22. (**B**) BFU-Es were infected with indicated viral shRNAs and cultured in the presence of 3 nM PD102807. Numbers of cells in the culture system were counted on day 6, and the mean and SD of relative fold expansion of 3 measurements from distinct samples are shown. (**C**) The knockdown efficiency of mouse *Kit* shRNAs is shown using western blots. Unprocessed blots are in fig. S22. (**D**) BFU-Es were infected with indicated viral shRNAs and cultured in the presence of 3 nM PD102807. Numbers of cells in the culture system were counted on day 6, and the mean and SD of relative fold expansion of 3 measurements from distinct samples are shown. All *P* values were calculated using the one-tailed t-test.

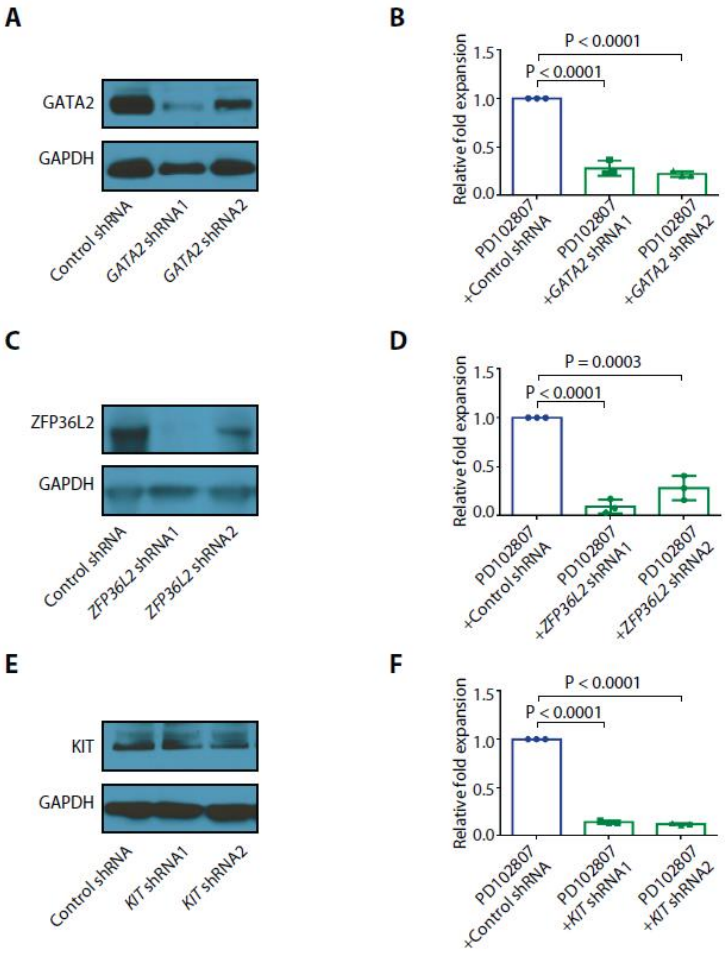


**Fig. S21. GATA2, ZFP36L2, and KIT function downstream of CHRM4 to regulate erythroid expansion in erythroid-cultured human CD34$^+$ cells.** (**A**) The knockdown efficiency of human *GATA2* shRNAs is shown using western blots. Unprocessed blots are in fig. S22. (**B**) Human CD34$^+$ cells were infected with indicated viral shRNAs and cultured in erythroid differentiation system with 3 nM PD102807. Numbers of cells in the culture system were counted on day 10, and the mean and SD of relative fold expansion of 3 measurements from distinct samples are shown. (**C**) The knockdown efficiency of human *ZFP36L2* shRNAs is shown using western blots. Unprocessed blots are in fig. S22. (**D**) Human CD34$^+$ cells were infected with indicated viral shRNAs and cultured in erythroid differentiation system with 3 nM PD102807. Numbers of cells in the culture system were counted on day 16, and the mean and SD of 3 measurements from distinct samples are shown. (**E**) The knockdown efficiency of human *KIT* shRNAs is shown using western blots. Unprocessed blots are in fig. S22. (**F**), Human CD34$^+$ cells were infected with indicated viral shRNAs and cultured in erythroid differentiation system with 3 nM PD102807. Numbers of cells in the culture system were counted on day 14, and the mean and SD of relative fold expansion of 3 measurements from distinct samples are shown. All *P* values were calculated using the one-tailed t-test.

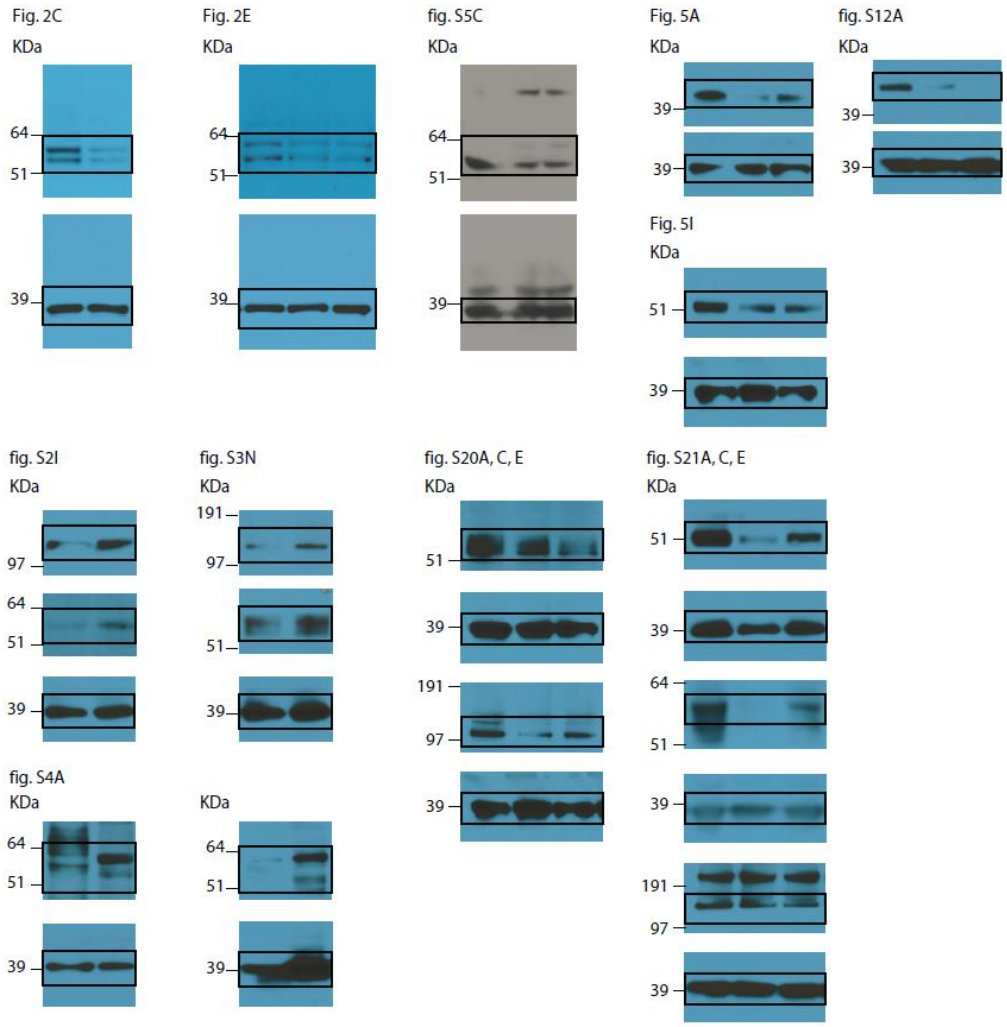


**Fig. S22. Unprocessed Western blots are shown.** Unprocessed western blots are provided for Fig. 2C, Fig. 2E, Fig. 5A, Fig. 5I, fig. S2I, fig. S3N, fig. S4A, fig. S5C, fig. S12A, fig. S20A, C, and fig. S21A, C, E.

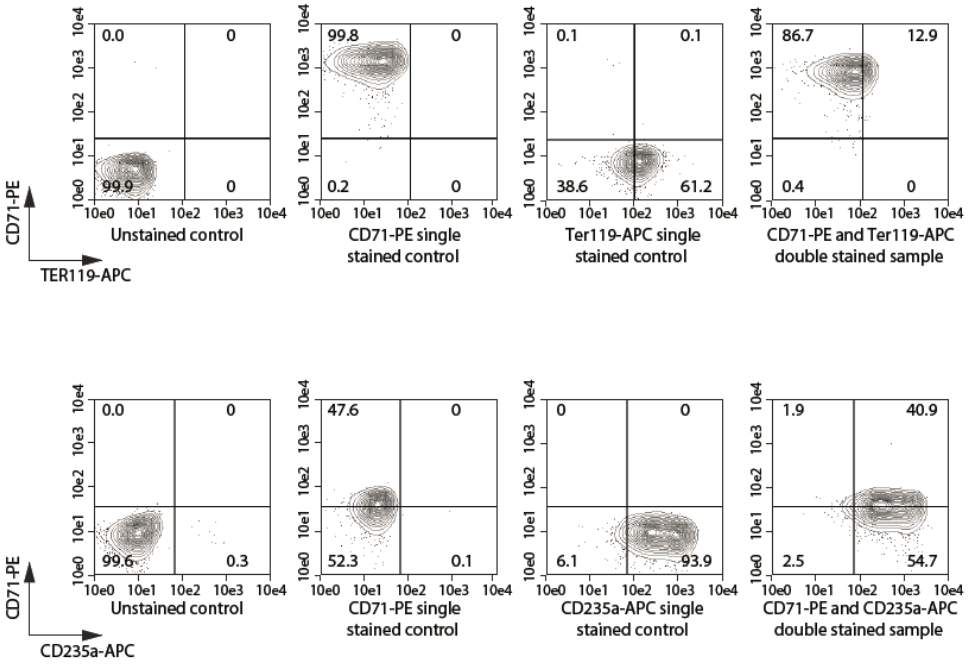


**Fig. S23. Flow cytometry control gating plots are shown.** Flow cytometry unstained control and single color stained control gating plots are provided for fig. S2E and fig. S3I and L.

**Table S1. $IC_{50}$ and $K_i$ values of PD102807 on indicated receptors.**

| Assay | $IC_{50}$ (M) | Ki (M) |
|---|---|---|
| **CHRM1** | >1.0E-05 | NA |
| **CHRM2** | 3.6E-06 | 2.5E-06 |
| **CHRM3** | 2.9E-07 | 2.0E-07 |
| **CHRM4** | 7.4E-09 | 4.6E-09 |
| **CHRM5** | >1.0E-05 | NA |
| **NMDA** | NA | NA |
| **Histamine H1** | NA | NA |

**Table S2. Clinical and molecular characteristics of the eight patients with MDS.**

| Sample ID | Age | 2016 WHO Classified-Subtype of MDS (*48*) | Cytogenetic and Molecular Alterations[1] |
|---|---|---|---|
| MDS-1 | 76 | MDS-EB-2 | Complex karyotype (del(3p), del (10q), add(12q), -13, Der(14)t(13;14), add(17p), del(20q) |
| MDS-2 | 79 | MDS-EB-2 | Del(5q) and monosomy 7, 18, and 22 |
| MDS-3 | 75 | MDS with multilineage dysplasia | Normal karyotype, *STAG2* A98fs*15 |
| MDS-4 | 59 | MDS-EB-1 | Trisomy 8, *JAK2*V617F/WT |
| MDS-5 | 73 | MDS-EB-2 | Deletion 5q |
| MDS-6 | 76 | MDS-EB-2 | Trisomy 8, RUNX1R107fs, TET2 T229fs |
| MDS-7 | 70 | MDS-EB-1 | Normal karyotype, *SF3B1*K666N, *CSF1R*T618I |
| MDS-8 | 64 | MDS-EB-2 | Normal karyotype (no mutations detected) |

[1]Genetic alterations were identified using a CLIA-certified 24 gene panel covering the most recurrently mutated genes in myeloid neoplasms (for patient MDS-2) or FoundationOne Heme (for patients MDS-3, MDS-4, and MDS-7) in addition to conventional FISH and karyotype (which was performed on all patients).